ACS OMEGA

Open Access

http://pubs.acs.org/journal/acsodf

Article

Production, Isolation, and Characterization of Stable Isotope-Labeled Standards for Mass Spectrometric Measurements of Oxidatively-Damaged Nucleosides in RNA

Pawel Jaruga,* Melis Kant, and Miral Dizdaroglu

Cite This: *ACS Omega* 2025, 10, 1519−1530

Read Online

ACCESS | Metrics & More | Article Recommendations | Supporting Information

ABSTRACT: RNA undergoes oxidatively induced damage in living organisms analogous to DNA. RNA is even more vulnerable to damage than DNA due to its greater abundance, single-strandedness, lack of repair and chromatin proteins shield, and instability, among other effects. RNA damage can adversely affect gene expression, leading to protein synthesis alterations, cell death, and other detrimental biological consequences. Growing indications suggest the involvement of oxidatively induced RNA damage in the pathogenesis of various human diseases, aging, and age-related diseases. Oxidatively induced damage can cause modifications to all four heterocyclic bases in RNA. Precise measurement of such modifications in RNA is essential for understanding the biological effects of oxidatively induced RNA damage. In the past, mass spectrometry has been used for this purpose. In mass spectrometric measurements, the use of stable isotope-labeled analogues of analytes as internal standards is essential for accurate quantifications. Past work utilized a stable isotope-labeled analogue of 8-hydroxyguanosine only as an internal standard. Thus, far, no stable isotope-labeled analogues of other oxidatively modified RNA nucleosides were available. In the present work, we report on the preparation, isolation, and characterization of the ^{13}C- and ^{15}N-labeled analogues of a variety of modified pyrimidine- and purine-derived RNA nucleosides. We also show the application of these internal standards for the measurement of oxidatively induced RNA damage in several commercially available RNA samples and in DNA along with DNA damage.

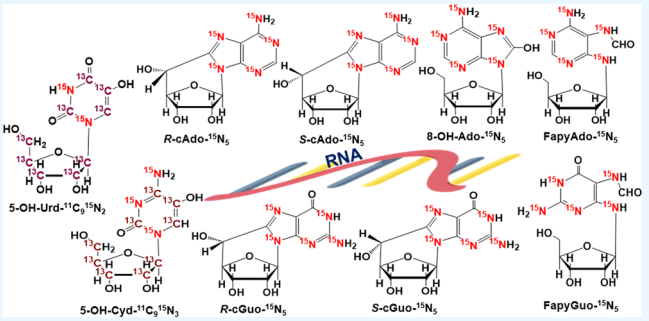

1. INTRODUCTION

In aerobic living organisms, oxygen-derived species, including free radicals, are continuously formed by regular intracellular metabolism and by exogenous sources such as ionizing radiations, UV radiation, redox-cycling drugs, carcinogenic compounds, environmental pollutants, etc. [reviewed in refs 1−4]. Oxygen metabolism produces hydroxyl radical (•OH), superoxide radical ($O_2^{\bullet-}$) and nonradical H_2O_2. Ionizing radiations also produce these species, an H atom (H•), a free radical, and a hydrated electron (e_{aq}^-) [reviewed in refs 1 and 3]. The hydroxyl radical is highly reactive, engaging with biological molecules at rates that approach the limits of diffusion-controlled kinetics [reviewed in refs 1, 3, and 4]. Interestingly, •OH has also been identified in the lower atmosphere (troposphere), contributing to the chemistry of this part of the atmosphere.[5,6] Reactions of •OH with DNA generate an overabundance of products from the heterocyclic DNA nucleobases and the 2′-deoxyribose moiety of DNA [reviewed in refs 3, 4, and 7]. This category of damage is referred to as oxidatively induced DNA damage, characterized by modifications to the DNA structure resulting from oxidative stress. The heterocyclic nucleobases and the ribose moiety in RNA can also undergo reactions with •OH and other reactive species leading to oxidatively induced RNA damage. In the past, however, this type of modification of RNA has received much less attention than that to DNA, although various types of RNA in different cellular components are more vulnerable to oxidatively induced damage than DNA due to more abundance of RNA than DNA, single-strandedness, and lack of repair among other factors.[8−25] Other numerous modifications also occur in RNA molecules as identified since the 1950s with the discovery of pseudouridine[26,27] and other modified nucleosides.[28−33] A summary of close to 100 modified nucleosides in RNA has been published.[34−36] Mass spectrometry has been widely used for the identification and characterization of modified RNA nucleosides.[37−40] The untargeted analysis by a DNA/RNA adductomics approach and the measurement of a variety of methylated purine nucleosides using mass spectrometry have also been

Received: October 11, 2024
Revised: December 2, 2024
Accepted: December 12, 2024
Published: December 21, 2024

https://doi.org/10.1021/acsomega.4c09310
ACS Omega 2025, 10, 1519−1530

demonstrated.[41,42] More developments in the field of the measurement of oxidatively induced DNA damage and RNA damage, among other types of damage, have been extensively reviewed.[43,44]

RNA modifications disturb translational accuracy, leading to adverse effects on protein synthesis. This can trigger cell deterioration, leading to cell death and other detrimental biological consequences. There is an increasing body of evidence indicating that RNA damage induced by oxidative stress plays a significant role in the pathogenesis of various human diseases, as well as in the processes of aging and age-related diseases.[16,19,24,33,45−68] The importance of the potential occurrence of oxidatively induced damage to RNA is related to its growing use in RNA-based therapeutics such as mRNA vaccines, antisense therapeutics, genome editing, RNA interference, RNA aptamers, microRNAs, RNA drugs, RNA editing, RNA modifications as biomarkers and others,.[33,66,69−81] Those processes require the application of adequate methodologies and securing proper quality control procedures. Ribonucleotides are inserted into DNA during replication by DNA polymerases, leading to genomic instability.[82−85] The presence of noncanonical ribonucleotides in DNA and the emerging significance of the involvement of RNA in the repair of DNA damage enhances the importance of RNA damage.[55,84−92] A recent report published in 2024 by the US National Academies of Sciences, Engineering, and Medicine emphasized the mounting evidence that RNA modifications can lead to a variety of human diseases and a better understanding and measurement of such modifications may result in targeted medical treatments.[93] Among the several key efforts suggested was also the development of standards for the measurement of RNA modifications.

In the past, oxidatively induced RNA damage was investigated using different methodologies (reviewed in ref 64). Employing liquid chromatography−tandem mass spectrometry (LC−MS/MS), hydroxyl radical-induced damage via ionizing radiation to polyadenylic acid as a model compound for RNA was shown to lead to the formation of 8-hydroxyadenosine (8-OH-Ado), 4-amino-5-formylamino-6-(ribosyl)aminopyrimidine (FapyAdo), (5′*R*)-8,5′-cycloadenosine (*R*-cAdo), and (5′*S*)-8,5′-cycloadenosine (*S*-cAdo).[94] In RNA, the most widely measured product was 8-hydroxyguanine (8-OH-Gua) (also named 8-oxoguanine) as its nucleoside form 8-hydroxyguanosine (8-OH-Guo) using a variety of analytical procedures and disease conditions, and, in some cases, together with the quantification of 8-hydroxy-2′-deoxyguanosine (8-OH-dG).[13,21,44,52,67,95−103] 8-OH-Gua is also one of the amplest products in oxidatively damaged DNA (reviewed in refs 3, 4, and 7). Other products such as 2-amino-4-hydroxy-5-formylamino-6-(ribosyl)aminopyrimidine (FapyGuo), FapyAdo, and 8-OH-Ado and an additional oxidation product of 8-OH-Gua, i.e., guanidinohydantoin, were also identified in RNA using LC−MS/MS.[21] The formation of the secondary product guanidinohydantoin was most likely due to the use of a very high level of the oxidizing agent.

In the previous measurements of the oxidatively induced RNA damage using mass spectrometry, no stable-isotope-labeled analogues of the analytes were used as internal standards except for 8-OH-Guo.[13,67] In some cases, it is not even clear as to how the quantifications had been achieved. In mass spectrometric measurements, it is essential to use stable isotope-labeled analogues of the analytes as internal standards for unequivocal identification and accurate quantification. In the present work, we report on the production, isolation, and characterization of ^{13}C- and ^{15}N-labeled analogues of a variety of the oxidatively damaged purine and pyrimidine nucleosides of RNA to be used as internal standards for the mass spectrometric measurement of oxidatively induced RNA damage.

2. RESULTS AND DISCUSSION

This work aimed to produce, isolate, and characterize the ^{13}C- and ^{15}N-labeled analogues of oxidatively induced RNA nucleosides as internal standards for the measurement of RNA damage in biological samples by mass spectrometry with isotope-dilution. To produce these compounds, we used our previously published procedures for the production and isolation of the stable isotope-labeled analogues of modified DNA nucleosides.[104−107] The samples of γ-irradiated Ado-$^{15}N_5$ and Guo-$^{15}N_5$ were analyzed by LC with UV-detection. Figure S1A,B shows the elution profiles of the LC analysis with UV detection of the modified nucleosides obtained from γ-irradiated Ado-$^{15}N_5$ and Guo-$^{15}N_5$, respectively. The collected areas of the effluents corresponding to each product are shown by green (starting point) and red (ending point) indicators. For the structural conformation, LC−MS/MS under the MS mode was used to individually record the total-ion mass spectra of the isolated compounds. Two peaks for FapyAdo-$^{15}N_5$ were observed, likely corresponding to the β and α anomers of the pyranose forms of this compound in aqueous solution in analogy to the anomers of FapydA identified in γ-irradiated 2′-deoxyadenosine,[104,108−112] with the β anomer of the pyranose forms eluting before the α-anomer of the pyranose forms on a reversed-phase column.[109] Previous studies have shown the epimerization of FapydAdo and FapydGuo from their furanose forms into their pyranose forms in an aqueous solution once released from DNA.[108−111] The pyranose form of these compounds is unattainable in DNA or RNA due to the 5′-protection of the furanose form.[108,109] Figure 1 shows the full-scan mass spectrum of FapyAdo-$^{15}N_5$, which exhibited a protonated molecular ion (MH^+) at m/z 291

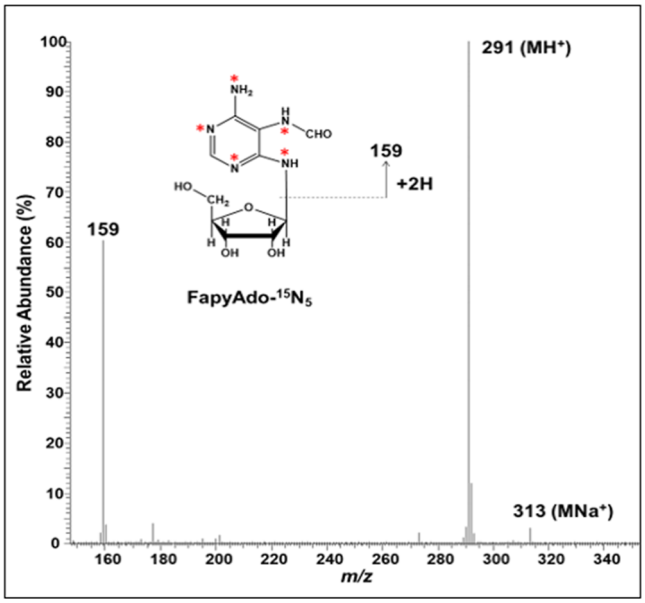

Figure 1. Full-scan mass spectrum of FapyAdo-$^{15}N_5$ (*denotes position of ^{15}N isotope).

https://doi.org/10.1021/acsomega.4c09310
ACS Omega 2025, 10, 1519−1530

as the base peak, a doubly protonated free base ion (BH_2^+) at m/z 159 and a sodium adduct ion (MNa^+) at m/z 313, as expected from the previously published mass spectra of unlabeled FapyAdo,[21,94] and FapydAdo.[104,109] FapyGuo-$^{15}N_5$ also yielded two peaks corresponding to its β- and α-pyranose forms in analogy to FapydA. Its full-scan mass spectrum is shown in Figure 2, which exhibited an MH^+ at m/z 307 as the base peak, a BH_2^+ at m/z 175 and an MNa^+ at m/z 329 in accordance with the mass spectrum of unlabeled FapyGuo.[21]

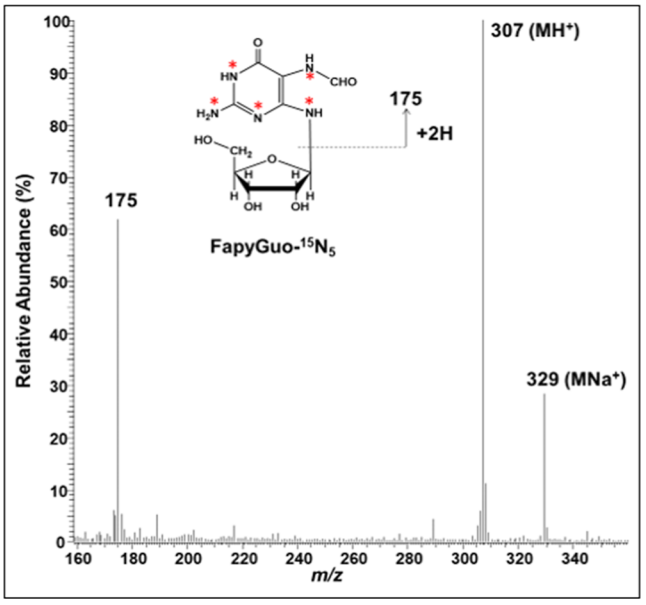

Figure 2. Full-scan mass spectrum of FapyGuo-$^{15}N_5$ (*denotes position of ^{15}N isotope).

The mass spectrum of 8-OH-Ado-$^{15}N_5$ consisted of an MH^+ at m/z 289 as the base peak, a BH_2^+ ion at m/z 157 and an MNa^+ at m/z 311 (Figure 3), agreeing with the previously published mass spectrum of unlabeled 8-OH-Ado.[21,94]

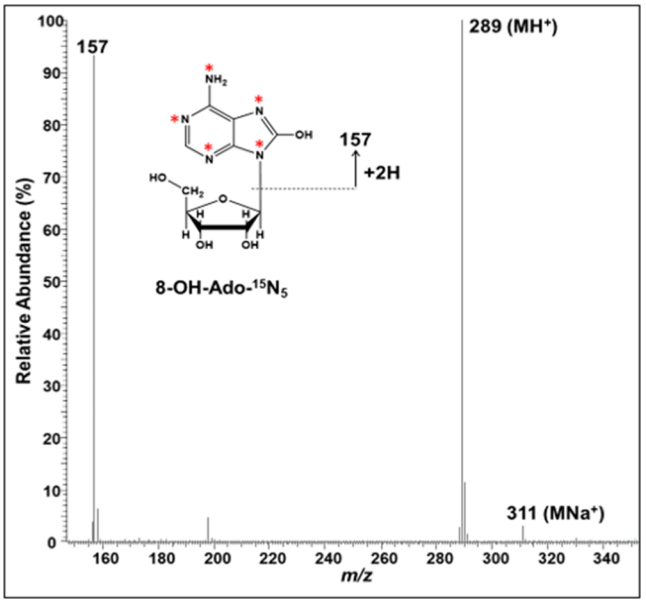

Figure 3. Full-scan mass spectrum of 8-OH-Ado-$^{15}N_5$ (*denotes position of ^{15}N isotope).

Similarly, the mass spectrum of the commercially available 8-OH-Guo-^{13}C,$^{15}N_2$ exhibited the corresponding ions at m/z 303 (MH^+) (base peak), m/z 171 (BH_2^+) and m/z 325 (MNa^+) (Figure 4). (5′*R*)-8,5′-cAdo-$^{15}N_5$ and (5′*S*)-8,5′-

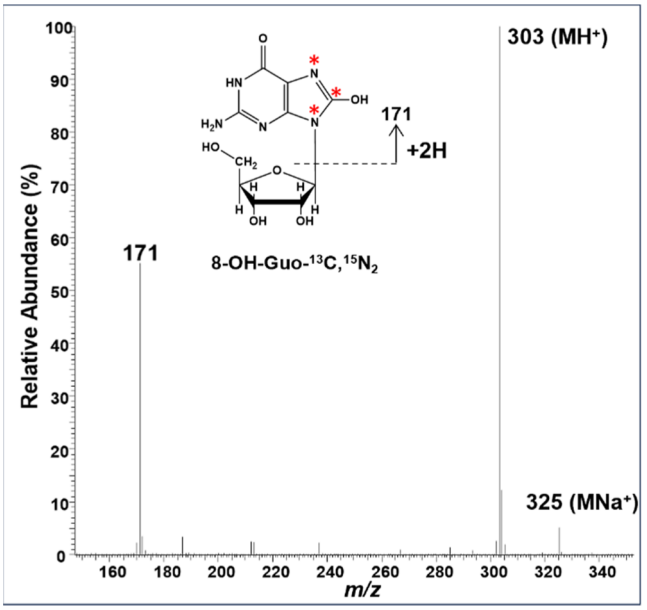

Figure 4. Full-scan mass spectrum of 8-OH-Guo-^{13}C,$^{15}N_2$ (*denotes position of ^{15}N isotope).

cAdo-$^{15}N_5$ exhibited identical mass spectra with an MH^+ at m/z 271 as the base peak, an MNa^+ at m/z 293 and an ion at m/z 169, which results from the simultaneous cleavage of the glycosidic bond and the bond between the 4′-carbon and 5′-carbon of the ribose moiety with an H atom transfer and contains the base moiety and the 5′-CHOH portion of the ribose moiety plus an H atom (Figures 5 and 6).[94,104,105] Similarly, the mass spectra of (5′*R*)-8,5′-cGuo-$^{15}N_5$ and (5′*S*)-8,5′-cGuo-$^{15}N_5$ had the corresponding ions at m/z 287 (MH^+),

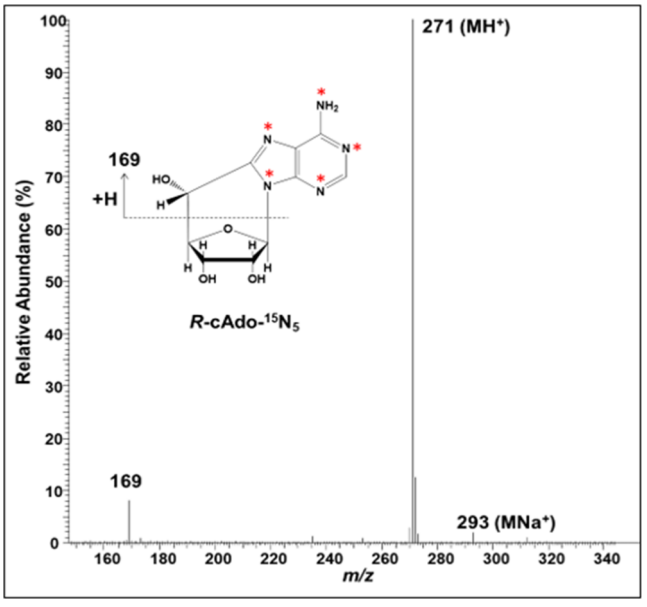

Figure 5. Full-scan mass spectrum of *R*-cAdo-$^{15}N_5$ (*denotes position of ^{15}N isotope).

https://doi.org/10.1021/acsomega.4c09310
ACS Omega 2025, 10, 1519−1530

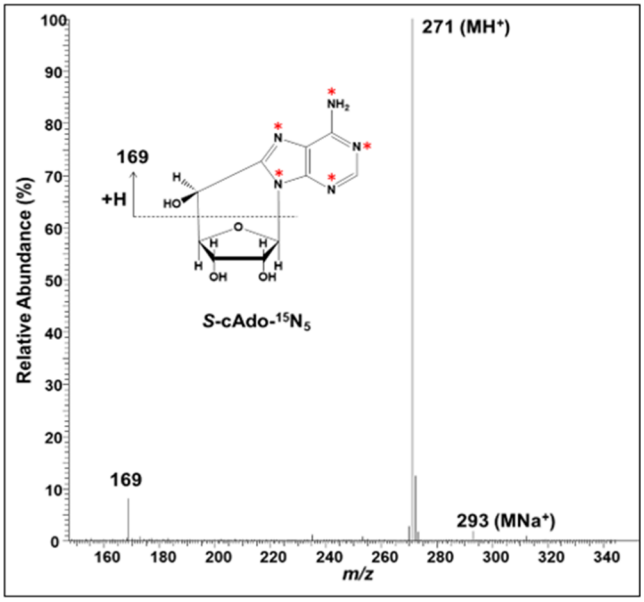

Figure 6. Full-scan mass spectrum of *S*-cAdo-$^{15}N_5$ (*denotes position of ^{15}N isotope).

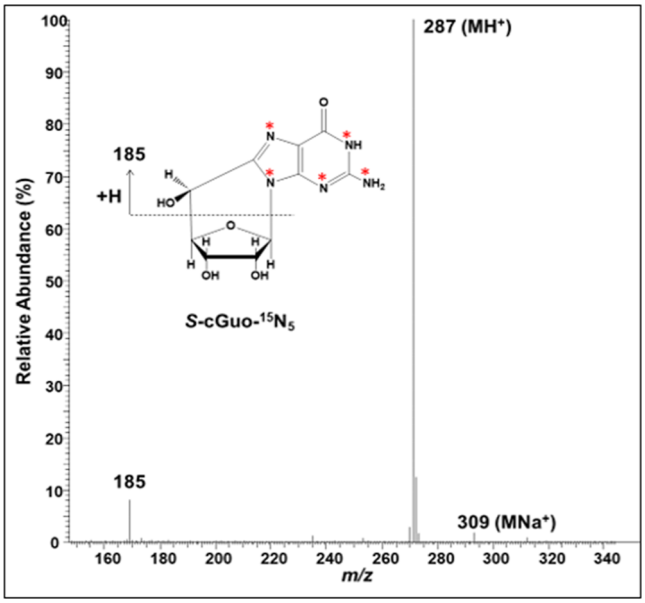

Figure 8. Full-scan mass spectrum of *S*-cGuo-$^{15}N_5$ (*denotes position of ^{15}N isotope).

m/z 309 (MNa^+) and m/z 185 (Figures 7 and 8). Next, the absorption spectra of the isolated compounds were recorded.

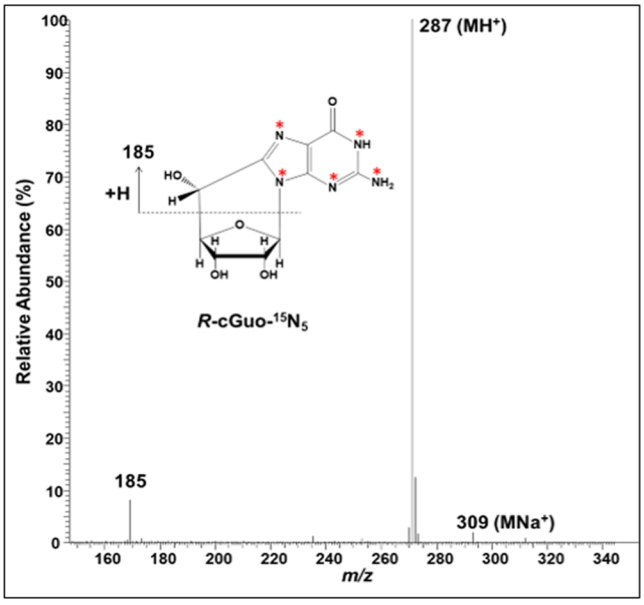

Figure 7. Full-scan mass spectrum of *R*-cGuo-$^{15}N_5$ (*denotes position of ^{15}N isotope).

The β- and α-anomers of FapyAdo-$^{15}N_5$ gave identical absorption spectra with a maximum at 262 nm (Supporting Information Figure S2). As expected, these absorption spectra were identical to that of 4,6-diamino-5-formamidopyrimidine (FapyAde).[113,114] Supporting Information Figure S3 shows the absorption spectrum of FapyGuo-$^{15}N_5$ with a maximum at 266 nm, which is essentially identical to the previously published spectrum of 2,6-diamino-4-hydroxy-5-formamidopyrimidine (FapyGua).[113] The absorption spectra *R*-cAdo-$^{15}N_5$ and *S*-cAdo-$^{15}N_5$ were identical with a maximum at 265 nm (Supporting Information Figure S4) in previously.[104,115,116] *R*-cGuo-$^{15}N_5$ and *S*-cGuo-$^{15}N_5$ exhibited identical absorption spectra (Supporting Information Figure S5) with the absorption maximum at 270 nm. The absorption spectrum of 8-OH-Ado-$^{15}N_5$ with a agreement with the absorption spectrum of the commercially available *S*-cAdo and that of cAdo published maximum at 268 nm (Supporting Information Figure S6) was similar to that of 8-hydroxyadenine (8-OH-Ade).[113] Two absorption maxima at 245 and 294 nm were observed in the absorption spectrum of 8-OH-Guo-$^{15}N_5$ (Supporting Information Figure S7) in agreement with that of 8-OH-dGuo identified in DNA.[117,118] The concentrations of the labeled compounds in their aqueous solutions were measured using their molar absorption coefficients (L mol^{-1} cm^{-1}) as follows: FapyAdo-$^{15}N_5$, 4700 at 262 nm, FapyGuo-$^{15}N_5$, 12,900 at 266 nm, 8-OH-Ado-$^{15}N_5$, 12,200 at 260 nm, 8-OH-Guo-^{13}C,$^{15}N_2$, 12,300 at 245 nm and 10,300 at 294 nm.[113,114,117] *R*-cAdo-$^{15}N_5$ and *S*-cAdo-$^{15}N_5$, 15,200 at 265 nm,[104] *R*-cGuo-$^{15}N_5$ and *S*-cGuo-$^{15}N_5$, 13,000 at 270 nm.[107]

5-OH-Cyd-$^{13}C_9$,$^{15}N_3$ and 5-OH-Urd-$^{13}C_9$,$^{15}N_2$ were collected using the analytical column. However, 5-OH-Cyd-$^{13}C_9$,$^{15}N_3$ and 5-OH-Urd-$^{13}C_9$$^{15}N_2$ could not be isolated in pure forms because of other coeluting compounds. The concentration of 5-OH-Cyd-$^{13}C_9$,$^{15}N_3$ in the collected fraction was measured by GC−MS/MS using the commercially available 5-OH-Cyt-^{13}C,$^{15}N_2$ as an internal standard. For this purpose, a known amount of the collection fraction containing 5-OH-Cyd-$^{13}C_9$,$^{15}N_3$ was mixed with a known amount of 5-OH-Cyt-^{13}C,$^{15}N_2$. The mixture was dried in a SpeedVac and then hydrolyzed with formic acid (60%) followed by lyophilization. The lyophilized sample was trimethylsilylated and analyzed by GC−MS/MS using the transition m/z 346 ($M^{+\bullet}$) → m/z 345 (M − $^{\bullet}H$) for the trimethylsilyl derivative (TMS) of 5-OH-Cyt-^{13}C,$^{15}N_2$, and the transition m/z 350 ($M^{+\bullet}$) → m/z 349 (M − $^{\bullet}H$) for the TMS derivative 5-OH-Cyt-$^{13}C_4$,$^{15}N_3$ under the experimental conditions described previously.[119] The concentration of 5-OH-Urd-$^{13}C_9$$^{15}N_2$ in the collected fraction was measured by LC−MS/MS using the commercially available 5-OH-Urd as an internal standard and the m/z 272 (MH^+) → m/z 135 (base + 2H) transitions for 5-

https://doi.org/10.1021/acsomega.4c09310
ACS Omega 2025, 10, 1519−1530

OH-Urd-$^{13}C_9$,$^{15}N_2$ and m/z 261 (MH^+) → m/z 129 (base + 2H) transitions for 5-OH-Urd.

The limit of quantification (LOQ) with a signal-to-noise ratio of 10 for each compound injected on the LC column was measured using the SRM mode of the MS/MS. They were as follows: 7 fmol of FapyAdo-$^{15}N_5$, 13 fmol of FapyGuo-$^{15}N_5$, 2.5 fmol of 8,5′-cAdo-$^{15}N_5$, 200 fmol of 8,5′-cGuo-$^{15}N_5$, 19 fmol of 8-OH-Guo-$^{15}N_3$ and 1.2 fmol of 8-OH-Ado-$^{15}N_5$, 1 fmol of 5-OH-Cyd-$^{13}C_9$,$^{15}N_3$, and 6 fmol of 5-OH-Urd-$^{13}C_9$,$^{15}N_2$. To validate the use of the isolated standards, we used RNA samples purchased from three different commercial sources to determine whether modified nucleosides can be identified and quantified. Aliquots of the isolated stable isotope-labeled internal standards were added to aliquots of RNA samples. Following hydrolysis of the RNA samples to nucleosides, the hydrolysates were analyzed by LC−MS/MS with SRM using the following m/z transitions:

m/z 286 → m/z 154 (FapyAdo), m/z 291 → m/z 159 (FapyAdo-$^{15}N_5$), m/z 302 → m/z 170 (FapyGuo), m/z 307 → m/z 175 (FapyGuo-$^{15}N_5$), m/z 260 → m/z 128 (5-OH-Cyd), m/z 272 → m/z 135 (5-OH-Cyd-$^{13}C_9$,$^{15}N_3$), m/z 261 → m/z 129 (5-OH-Urd), m/z 272 → m/z 135 (5-OH-Urd-$^{13}C_9$,$^{15}N_2$), m/z 266 → m/z 164 (*R*-cAdo and *S*-cAdo), m/z 271 → m/z 169 (*R*-cAdo-$^{15}N_5$ and *S*-cAdo-$^{15}N_5$), m/z 282 → m/z 180 (*R*-cGuo and *S*-cGuo), m/z 287 → m/z 185 (*R*-cGuo-$^{15}N_5$) and (*S*-cGuo-$^{15}N_5$), m/z 300 → m/z 168 (8-OH-Guo), m/z 303→ m/z 171 (8-OH-Guo-^{13}C,$^{15}N_2$), m/z 284 → m/z 152 (8-OH-Ado), m/z 289 → m/z 157 (8-OH-Ado-$^{15}N_5$). Figure 9 shows an example of ion-current profiles of the m/z transitions of the RNA modified nucleosides and their stable isotope-labeled analogues as internal standards, recorded during the analysis of a hydrolyzed RNA sample. As indicated above, the β- and α-pyranose forms of both FapydAdo and FapydGuo were observed. In addition, we wished to find out whether DNA samples would contain RNA nucleoside lesions, which may be formed by modification of ribonucleotides introduced into DNA by DNA polymerases (reviewed in refs 88 and 89). Aliquots of a commercially available calf thymus DNA sample were mixed with the aliquots of the stable isotope-labeled RNA standards. To simultaneously check some modified DNA nucleosides for comparison, stable isotope-labeled DNA standards *R*-cdA-$^{15}N_5$, *S*-cdA-$^{15}N_5$, *R*-cdG-$^{15}N_5$ and *S*-cdG-$^{15}N_5$, and 8-OH-dG-$^{15}N_5$ were also added. DNA samples were hydrolyzed to nucleosides and then analyzed by LC−MS/MS with SRM using the m/z transitions listed above for the modified RNA nucleosides, and the following m/z transitions for the modified DNA nucleosides: m/z 250 → m/z 164 (*R*-cdA and *S*-cdA), m/z 255 → m/z 169 (*R*-cdA-$^{15}N_5$ and *S*-cdA-$^{15}N_5$), m/z 266 → m/z 180 (*R*-cdG and *S*-cdG), m/z 271 → m/z 185 (*R*-cdG-$^{15}N_5$ and *S*-cdG-$^{15}N_5$), m/z 284 → m/z 168 (8-OH-dG), m/z 289 → m/z 173 (8-OH-dG-$^{15}N_5$).[120,121] Figure 10 shows the measured levels of the modified RNA nucleosides in three commercially available RNAs purchased from different merchants. Intense levels of some of the modified nucleosides were observed. 8-OH-Guo had the highest level in all three RNAs.

Figure 11 shows the levels of modified RNA nucleosides in calf thymus DNA that were readily detectable. These results unequivocally demonstrate, for the first time, the presence of oxidatively modified RNA nucleosides in DNA. The incorporation of noncanonical ribonucleotides into DNA by DNA polymerases is well-known.[82−85] However, the modification of incorporated RNA nucleosides in DNA has not been shown previously. As a comparison, the levels of modified DNA nucleosides, which were measured simultaneously in the same DNA samples, are shown in Figure 12. The levels of DNA base lesions in calf thymus DNA separately measured by GC−MS/MS are given in Figure 13.

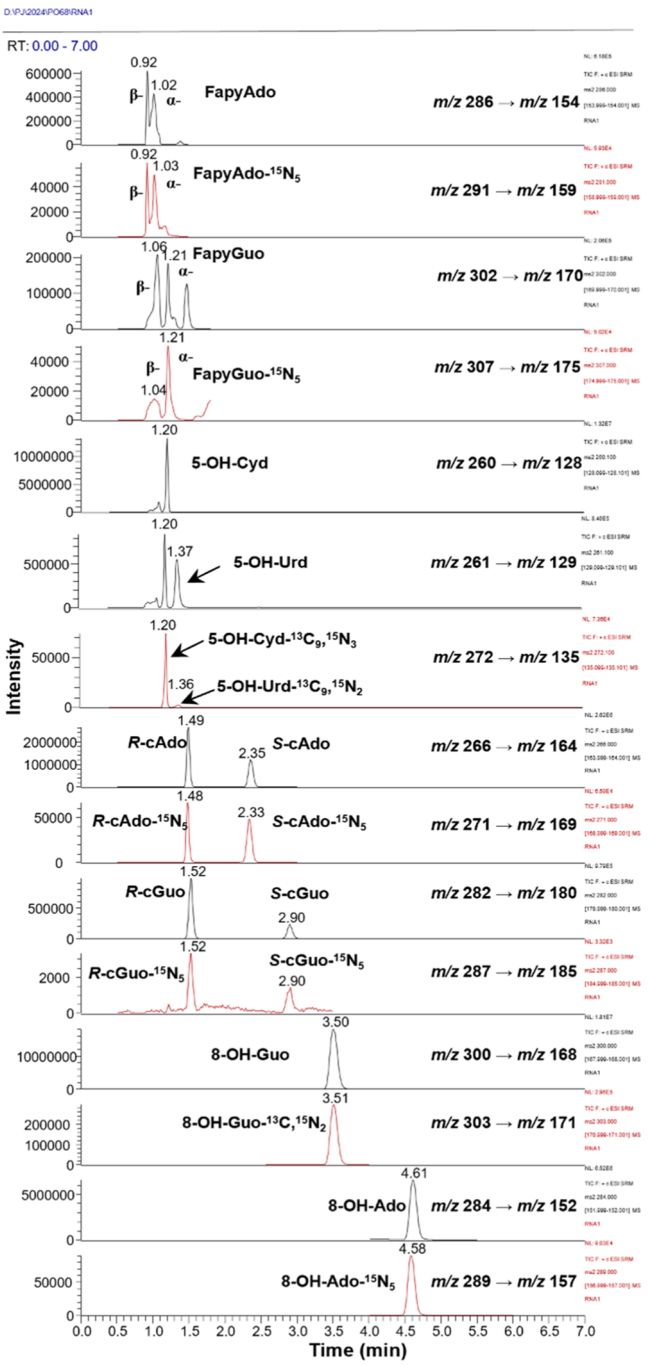

Figure 9. Ion-current profiles of the m/z transitions of modified RNA nucleosides and their stable isotope-labeled analogues as internal standards recorded during the analysis by LC−MS/MS with SRM of the hydrolysate of an RNA sample. Note that 5-OH-Cyd-$^{13}C_9$,$^{15}N_3$ and 5-OH-Urd-$^{13}C_9$,$^{15}N_2$ undergo the same transition: m/z 272 → m/z 135.

3. CONCLUSIONS

We produced, isolated, and characterized the stable isotope-labeled analogues of purine- and pyrimidine-derived lesions of

https://doi.org/10.1021/acsomega.4c09310
ACS Omega 2025, 10, 1519−1530

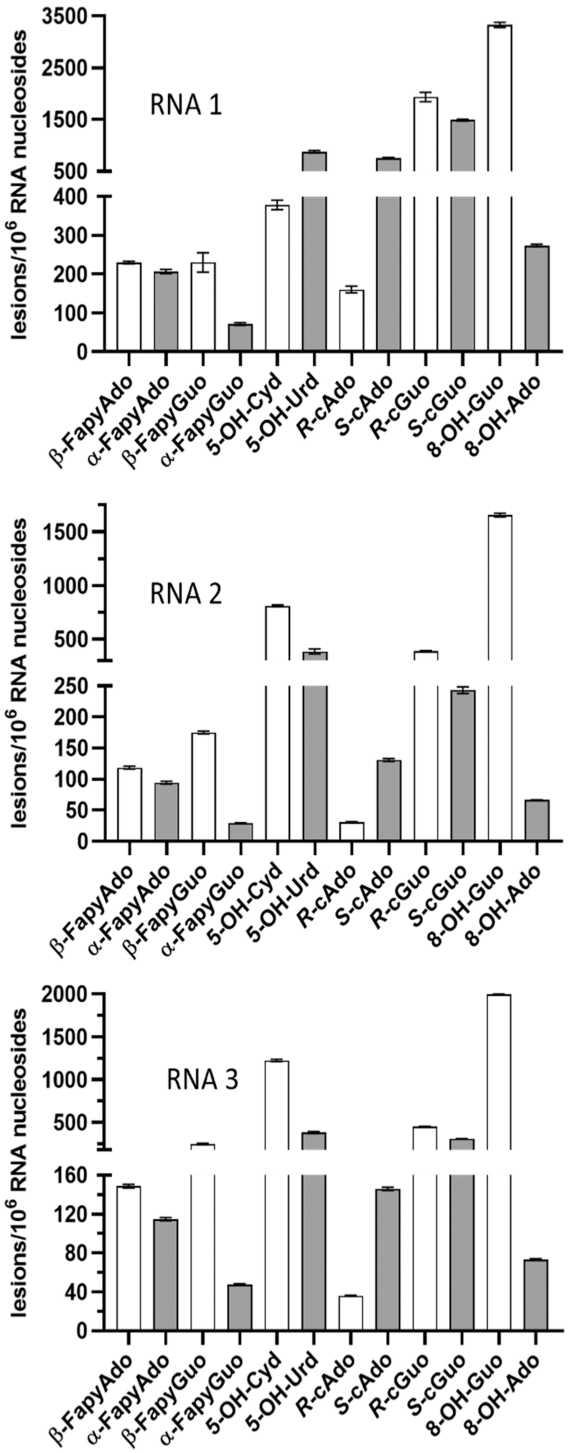

Figure 10. Levels of modified RNA nucleosides in RNA. Uncertainties are standard deviations, $n = 3$.

RNA nucleosides to be used as internal standards for the accurate identification and quantification of oxidatively induced RNA damage. We demonstrated, for the first time, the measurement of a variety of modified pyrimidine and purine nucleosides in RNA samples using these stable isotope-labeled internal standards. Moreover, we showed, also for the first time, the measurement of modified pyrimidine and purine nucleosides of RNA in DNA, along with some modified DNA nucleosides. The RNA and DNA samples used in the present work were commercially available ones. In future studies, the

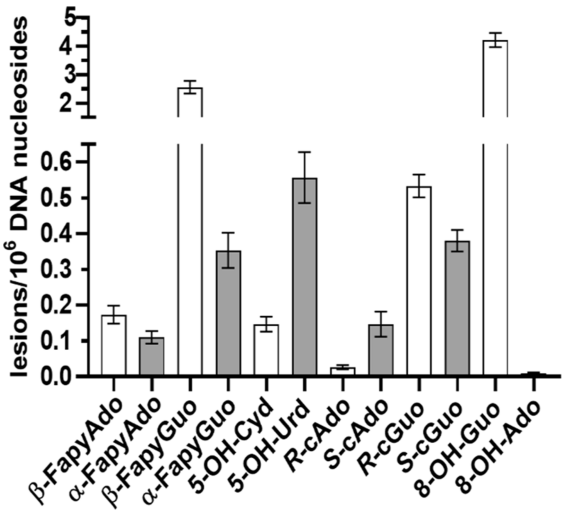

Figure 11. Levels of modified RNA nucleosides in calf thymus DNA. Uncertainties are standard deviations, $n = 3$.

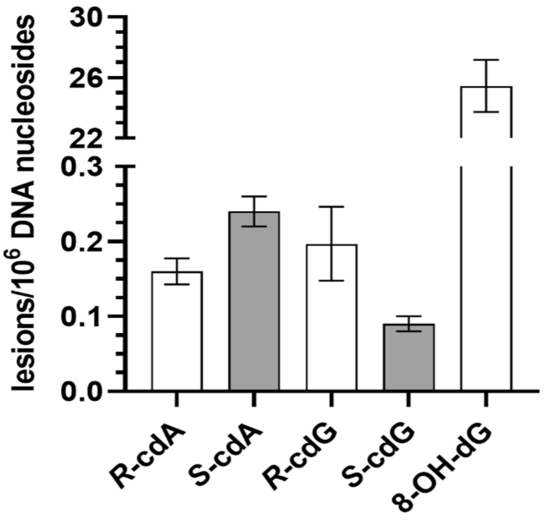

Figure 12. Levels of modified DNA nucleosides in calf thymus DNA. Uncertainties are standard deviations, $n = 3$.

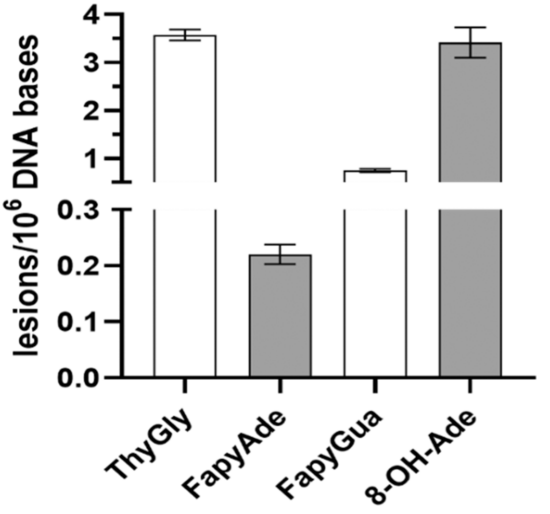

Figure 13. Quantities of modified DNA bases in calf thymus DNA. Uncertainties are standard deviations, $n = 3$.

https://doi.org/10.1021/acsomega.4c09310
ACS Omega 2025, 10, 1519−1530

isolated stable isotope-labeled standards may be used for the accurate measurement by mass spectrometry of modified RNA nucleosides in RNA as well as in DNA of biologically relevant samples, and biological fluids such as urine.

4. MATERIALS AND METHODS

4.1. Materials. Phosphodiesterase I and calf thymus DNA were bought from Sigma-Aldrich Chemical Co. (St. Louis, MO, USA). Yeast RNA samples were purchased from Roche Diagnostics Corporation (Indianapolis, IN, USA), European Pharmacopoeia Reference Standard/Krackeler Scientific (Albany, NY, USA) and Sigma-Aldrich (St Louis, MO, USA). Nuclease P1 was obtained from US Biological (Salem, MA, USA). Alkaline phosphatase was purchased from Roche Diagnostics Corporation (Indianapolis, IN, USA). Water with 0.1% (v/v) formic acid and acetonitrile with 0.1% (v/v) formic acid (both mass spectrometry-grade) were purchased from Thermo Fisher Scientific (Waltham, MA, USA). Adenosine-$^{15}N_5$ (Ado-$^{15}N_5$) and guanosine-$^{15}N_5$ (Guo-$^{15}N_5$) were purchased from Medical Isotopes Inc. (Pelham, NH, USA). 8-Hydroxyguanosine-^{13}C,$^{15}N_2$ (8-OH-Guo-^{13}C,$^{15}N_2$) was obtained from Toronto Research Chemicals (Toronto, ON, Canada). Cytidine-5′-monophosphate-$^{13}C_9$,$^{15}N_3$ ammonium salt (CMP-$^{13}C_9$,$^{15}N_3$), uridine-5′-monophosphate-$^{13}C_9$,$^{15}N_2$ ammonium salt (UMP-$^{13}C_9$,$^{15}N_2$), 8-hydroxy-2′-deoxyguanosine-$^{15}N_5$ (8-OH-dG-$^{15}N_5$) and 5-hydroxycytosine-^{13}C,$^{15}N_2$ (5-OH-Cyt-^{13}C,$^{15}N_2$) were purchased from Cambridge Isotope Laboratories (Andover, MA, USA). 5-Hydroxyuridine (5-OH-Urd) was purchased from Smolecule, Inc. (Pasadena, CA, USA). (5′*S*)-8,5′-Cycloadenosine (*S*-cAdo) was obtained from Berry & Associates, Inc. (Ann Arbor, MI, USA). Nanosep centrifugal devices 3K Omega Pall Lab were purchased from VWR (Radnor, PA, USA). Reverse osmose water purified through Thermo Scientific Barnstead GenePure Water Purification System (Waltham, MA, USA) was used for all other than LC applications.

4.2. Preparation of Stable Isotope-Labeled Compounds. The only commercially available stable isotope-labeled analogue of a modified RNA nucleoside was 8-OH-Guo-^{13}C,$^{15}N_2$. Stable isotope-labeled analogues of 8-OH-Ado, FapyAdo, *R*-cAdo, *S*-cAdo, FapyGuo, (5′*R*)-8,5′-cycloguanosine (*R*-cGuo), (5′*S*)-8,5′-cycloguanosine (*S*-cGuo), 5-hydroxycytidine (5-OH-Cyd), and 5-OH-Urd were not commercially available. To prepare these compounds, the aqueous solutions of commercially available Ado-$^{15}N_5$, Guo-$^{15}N_5$, CMP-$^{13}C_9$,$^{15}N_3$, and UMP-$^{13}C_9$,$^{15}N_2$ (5 mg each in 40 mL of water) were bubbled with N_2O for 1 h and then γ-irradiated in a ^{60}Co γ-source at a dose of 400 Gy (dose rate, 5.53 Gy/min) as previously described for the isolation of stable isotope-labeled analogues of modified DNA nucleosides.[104−107] Based on the known effects of ionizing radiation on nucleic acid components,[3,104−107,116] this treatment was expected to produce the modified RNA nucleosides mentioned above. The irradiated solutions were lyophilized to dryness. For dephosphorylation of CMP-$^{13}C_9$,$^{15}N_3$ and UMP-$^{13}C_9$,$^{15}N_2$ irradiation products, the dried compounds were dissolved in 1 mL of 10 mmol/L phosphate buffer (pH 8.0) and incubated with alkaline phosphatase (5 units) at 37 °C for 24 h. The samples were filtered using ultrafiltration membranes with a molecular mass cutoff of 3 kDa by centrifugation at 11,000*g* for 45 min at 10 °C. The internal standards (5′*R*)-8,5′-cyclo-2′-deoxyadenosine-$^{15}N_5$ (*R*-cdA-$^{15}N_5$), (5′*S*)-8,5′-cyclo-2′-deoxyadenosine-$^{15}N_5$ (*S*-cdA-$^{15}N_5$), (5′*R*)-8,5′-cyclo-2′-deoxyguanosine-$^{15}N_5$ (*R*-cdG-$^{15}N_5$), and (5′*S*)-8,5′-cyclo-2′-deoxyguanosine-$^{15}N_5$ (*S*-cdG-$^{15}N_5$) were produced and isolated as previously described.[105,107]

4.3. Preparation of RNA and DNA Samples. Both types of nucleic acids were dissolved in 25 mL of mass spectrometry-grade water at the concentration of 0.350 mg/mL. Concentrations were measured using NanoDropOne^C, Thermo Scientific (Waltham, MA, USA). Dissolved RNAs and DNA were placed in the dialysis tubes (Spectra/Por 7 Dialysis Membrane, Pretreated RC Tubing, MWCO: 2 kDa, Repligen, Waltham, MA, USA) and dialyzed against LC−MS grade water changed 3 times for 6 h at 4 °C. After dialysis, nucleic acid concentration was measured again, and samples for analysis were aliquoted 50 μg each into 1.5 mL DNase/RNase free tubes and dried in speed-vac.

4.4. Identification of Modified RNA Nucleosides in Irradiated Samples by Liquid Chromatography−Tandem Mass Spectrometry. Aliquots (5 μL) of irradiated samples of Ado-$^{15}N_5$ and Guo-$^{15}N_5$ were analyzed using a Thermo TSQ Altis Triple Stage Quadrupole MS/MS system with a vanquish flex quaternary ultrahigh-performance liquid chromatography (UHPLC) front-end system equipped with a diode array UV detector (Thermo Fisher Scientific, Waltham, MA), and a Supelcosil LC-8-DB semipreparative column (25 cm × 10 mm, particle size 5 μm) (MilliporeSigma, Burlington, MA) connected to the MS/MS. The effluents were divided by a flow-splitter in a 4-to-1 ratio with a flow rate of 1.5 mL/min to the UV detector monitoring eluted fractions at λ = 260 nm, and with a flow rate of 0.5 mL/min to the MS/MS (Supporting Information Figure S8). The column temperature was kept at 30 °C. The MS/MS parameters were as follows: spray voltage = 3.5 kV; tube lens offsets = 89 V for Q1 and Q3; vaporizer temperature = 275 °C; ion transfer tube temperature = 325 °C; sheath gas (nitrogen) pressure = 50 (arbitrary units); auxiliary gas (nitrogen) pressure = 10 (arbitrary units); sweep gas 2 (arbitrary units); collision gas (argon) pressure = 2.67 × 10^{-5} Pa (2 mTorr). Selected reaction monitoring (SRM) data were acquired in the positive ionization mode at a cycle time of 0.45 s, a Q1 resolution (full width at half-maximum, fwhm) of 0.7, a Q3 resolution (fwhm) of 1.2 and a chromatographic peak with 7 s. For the identification of the products of Ado-$^{15}N_5$ and Guo-$^{15}N_5$, the SRM scans were performed using the following mass/charge (m/z) transitions expected on the basis of the known fragmentation patterns of the nucleosides.[21,94,104,105,109,122] m/z 289 → m/z 157 (8-OH-Ado-$^{15}N_5$), m/z 291 → m/z 159 (FapyAdo-$^{15}N_5$), m/z 271 → m/z 169 (*R*-cAdo-$^{15}N_5$) and *S*-cAdo-$^{15}N_5$), m/z 307 → m/z 175 (FapyGuo-$^{15}N_5$), m/z 287 → m/z 185 (*R*-cGuo-$^{15}N_5$ and (*S*-cGuo-$^{15}N_5$). Irradiated and dephosphorylated samples of CMP-$^{13}C_9$$^{15}N_3$ and UMP-$^{13}C_9$$^{15}N_2$ were analyzed using the analytical column as described below and the following m/z transitions for identification: m/z 272 → m/z 135 (5-OH-Cyd-$^{13}C_9$,$^{15}N_3$) and m/z 272 → m/z 135 (5-OH-Urd-$^{13}C_9$,$^{15}N_2$). These compounds were separated from each other. Since m/z transitions were the same for both compounds, commercially available 5-OH-Urd was used for the distinction between them.

4.5. Isolation and Collection of Modified RNA Nucleosides by Liquid Chromatography. Modified purine nucleosides were collected using an Agilent liquid chromatograph 1100 equipped with a fraction collector (Agilent Technologies, Wilmington, DE) and a Supelcosil LC-8-DB semipreparative column (25 cm × 10 mm, particle size 5 μm)

https://doi.org/10.1021/acsomega.4c09310
ACS Omega 2025, 10, 1519−1530

(MilliporeSigma, Burlington, MA). The solvents A and B were water with 0.1% of formic acid plus 2% of acetonitrile and acetonitrile with 0.1% formic acid, respectively. A gradient from 0% of solvent B up to 11% in 18 min was used. The flow rate was 2 mL/min. The autosampler and column temperatures were kept at 6 and 40 °C, respectively. After each analysis, the solvent B was maintained at 90% for 7 min and then at 0% for 25 min to equilibrate the column. All collected fractions were dried in a SpeedVac concentrator (Savant, SPD2010, Thermo Fisher Scientific, Waltham, MA). 5-OH-Cyd-$^{13}C_9$,$^{15}N_3$ and 5-OH-Urd-$^{13}C_9$,$^{15}N_2$ were collected using the analytical column under the conditions described below.

4.6. Analysis of Isolated Modified Nucleosides. The isolated compounds were individually analyzed by LC−MS/MS under MS mode to record their full-scan mass spectra. The MS/MS conditions were as described above. A Zorbax Sb-Aq narrow-bore LC column (2.1 × 150 mm, 3.5 μm particle size) (Agilent Technologies, Wilmington, DE) with an attached Agilent Eclipse XDB-C8 guard column (2.1 × 12.5 mm, 5 μm particle size) was used. The column temperature was kept at 30 °C. Mobile phase A was water, and mobile phase B was acetonitrile, both containing 0.1% formic acid (v/v). A gradient of 2−10% of B/min in 5 min was used with a flow rate of 0.5 mL/min. After 5 min, B was increased to 90% in 0.1 min and kept at this level for 2 min and then another 10 min at 2% to equilibrate the column. Full scan mass spectra were acquired at a range of m/z 100−600 with a chromatographic peak width of 6 s, a scan rate of 1000 Da/s, and a Q1 resolution (fwhm) of 0.7. SRM conditions were used as described above.

4.7. Measurement of the UV Absorption Spectra of the Isolated Compounds. The absorption spectra of the isolated compounds were recorded using a Nanodrop One^C (Thermo Fisher Scientific, Waltham, MA).

4.8. Hydrolysis of RNA and DNA Samples, and Analysis of the Hydrolysates. Aliquots of 8-OH-Ado-$^{15}N_5$ (0.63 pmol), FapyAdo-$^{15}N_5$ (3.27 pmol), *R*-cAdo-$^{15}N_5$ (0.61 pmol), *S*-cAdo-$^{15}N_5$ (4.80 pmol), FapyGuo-$^{15}N_5$ (3.56 pmol), *R*-cGuo-$^{15}N_5$ (0.95 pmol), *S*-cGuo-$^{15}N_5$ (1.15 p mol), 8-OH-Guo-^{13}C,$^{15}N_2$ (8.60 pmol), 5-OH-Cyd-$^{13}C_9$,$^{15}N_3$ (0.33 pmol), and 5-OH-Urd-$^{13}C_9$,$^{15}N_2$ (0.07 pmol) were added to the 50 μg aliquots of RNA samples from three different sources and calf thymus DNA. In addition, the aliquots of the following internal standards were added to the DNA samples: *R*-cdA-$^{15}N_5$, *S*-cdA-$^{15}N_5$, *R*-cdG-$^{15}N_5$, *S*-cdG-$^{15}N_5$, and 8-OH-dG-$^{15}N_5$. Three replicates of RNA and DNA samples were used. The samples were dried in a SpeedVac at room temperature and then dissolved in 60 μL of 10 mmol/L tris-HCl (pH 7.5), containing 45 mmol/L $ZnCl_2$, and supplemented with 2.5 μL of 1 mol/L Na-acetate. The samples were incubated with nuclease P1 (1 unit), phosphodiesterase I (0.001 units), and alkaline phosphatase (5 units) at 37 °C for 18 h. After hydrolysis, the samples were filtered using ultrafiltration membranes with a molecular mass cutoff of 3 kDa by centrifugation at 12,000*g* for 30 min at 10 °C. Aliquots (50 μL) of these samples were analyzed by LC−MS/MS with SRM using the m/z transitions of the modified RNA nucleosides under the experimental conditions described above. The m/z transitions used for the measurement of modified DNA nucleosides and their internal standards were as previously described.[119]

4.9. Measurement of the DNA Nucleobase Lesions in Calf Thymus DNA. The levels of DNA nucleobase lesions thymine glycol (ThyGly), 4,6-diamino-5-formamidopyrimidine (FapyAde), 2,6-diamino-4-hydroxy-5-formamidopyrimidine (FapyGua), and 8-hydroxyadenine (8-OH-Ade) were quantified in calf thymus DNA by GC−MS/MS with isotope-dilution. The reason is that these modified bases can only be measured by GC−MS/MS using their stable isotope-labeled internal standards. There are no stable isotope-labeled analogues of these compounds as 2′-deoxynucleosides in our laboratory to be measured by LC−MS/MS. On the contrary, *R*-cdA, *S*-cdA, *R*-cdG, and *S*-cdG can only be measured by LC−MS/MS using their stable isotope-labeled internal standards, which exist in our laboratory as described above. 8-OH-dG was measured by LC−MS/MS using its available stable isotope-labeled internal standard along with *R*-cdA, *S*-cdA, *R*-cdG, and *S*-cdG in the same samples.

Three replicates of DNA samples were treated with two DNA glycosylases NTHL1 (a gift from Prof. Sylvie Doublié, Department of Microbiology and Molecular Genetics, Larner College of Medicine, The University of Vermont) and *Escherichia coli* Fpg (New England Biolabs) to remove these lesions from DNA. This was followed by trimethylsilylation and GC−MS/MS analysis using the m/z transitions as previously described.[119]

■ ASSOCIATED CONTENT

Supporting Information

The Supporting Information is available free of charge at https://pubs.acs.org/doi/10.1021/acsomega.4c09310.

Additional experimental details, and data (PDF)

■ AUTHOR INFORMATION

Corresponding Author

Pawel Jaruga − *Biomolecular Measurement Division, National Institute of Standards and Technology, Gaithersburg, Maryland 20899, United States;* orcid.org/0000-0001-9192-6084; Email: pawel.jaruga@nist.gov

Authors

Melis Kant − *Biomolecular Measurement Division, National Institute of Standards and Technology, Gaithersburg, Maryland 20899, United States;* Present Address: Biosystems and Biomaterials Division, National Institute of Standards and Technology, Gaithersburg, MD 20899, United States

Miral Dizdaroglu − *Biomolecular Measurement Division, National Institute of Standards and Technology, Gaithersburg, Maryland 20899, United States;* orcid.org/0000-0003-0283-1695

Complete contact information is available at: https://pubs.acs.org/10.1021/acsomega.4c09310

Author Contributions

P.J., M.K., and M.D. contributed equally to this work. All authors have read and agreed to the submitted version of the manuscript.

Funding

This work was supported by the National Institute of Standards and Technology.

Notes

The authors declare no competing financial interest.

■ ACKNOWLEDGMENTS

Certain equipment, instruments, software, or materials, commercial or noncommercial, are identified in this paper to adequately specify the experimental procedure. Such identification is not intended to imply recommendation or endorsement of any product or service by NIST, nor does it imply that the materials or equipment identified are necessarily the best available for the purpose.

■ DEDICATION

We dedicate this work to the memory of extraordinary scientist, NIST Fellow Dr. Miral Dizdaroglu, who sadly passed away on Dec 13th, 2024, during the last days of this article completion and whose insightful guidance was invaluable to this project. We are deeply grateful for the friendship and contributions of Dr. Dizdaroglu, one of the world's leading researchers in the field of DNA damage and repair, whose legacy continues to inspire us.

■ REFERENCES

(1) Halliwell, B.; Gutteridge, J. M. C. *Free Radicals in Biology & Medicine*; Oxford University Press, 2015.
(2) Halliwell, B. Understanding mechanisms of antioxidant action in health and disease. *Nat. Rev. Mol. Cell Biol.* **2024**, *25*, 13−33.
(3) von Sonntag, C. *Free-Radical-Induced DNA Damage and Its Repair*; Springer, 2006.
(4) Halliwell, B.; Adhikary, A.; Dingfelder, M.; Dizdaroglu, M. Hydroxyl radical is a significant player in oxidative DNA damage in vivo. *Chem. Soc. Rev.* **2021**, *50* (15), 8355−8360.
(5) Levy, H. Normal atmosphere: large radical and formaldehyde concentrations predicted. *Science* **1971**, *173* (3992), 141−143.
(6) Heald, C. L.; Kroll, J. H. A radical shift in air pollution. *Science* **2021**, *374* (6568), 688−689.
(7) Dizdaroglu, M.; Jaruga, P. Mechanisms of free radical-induced damage to DNA. *Free Radical Res.* **2012**, *46* (4), 382−419.
(8) Fiala, E. S.; Conaway, C. C.; Mathis, J. E. Oxidative DNA and RNA damage in the livers of Sprague-Dawley rats treated with the hepatocarcinogen 2-nitropropane. *Cancer Res.* **1989**, *49* (20), 5518−5522.
(9) Yanagawa, H.; Ogawa, Y.; Ueno, M. Redox ribonucleosides. Isolation and characterization of 5-hydroxyuridine, 8-hydroxyguanosine, and 8-hydroxyadenosine from Torula yeast RNA. *J. Biol. Chem.* **1992**, *267* (19), 13320−13326.
(10) Warner, W. G.; Wei, R. R. In vitro photooxidation of nucleic acids by ultraviolet A radiation. *Photochem. Photobiol.* **1997**, *65* (3), 560−563.
(11) Barciszewski, J.; Barciszewska, M. Z.; Siboska, G.; Rattan, S. I.; Clark, B. F. Some unusual nucleic acid bases are products of hydroxyl radical oxidation of DNA and RNA. *Mol. Biol. Rep.* **1999**, *26* (4), 231−238.
(12) Shen, Z.; Wu, W.; Hazen, S. L. Activated leukocytes oxidatively damage DNA, RNA, and the nucleotide pool through halide-dependent formation of hydroxyl radical. *Biochemistry* **2000**, *39* (18), 5474−5482.
(13) Weimann, A.; Belling, D.; Poulsen, H. E. Quantification of 8-oxo-guanine and guanine as the nucleobase, nucleoside and deoxynucleoside forms in human urine by high-performance liquid chromatography-electrospray tandem mass spectrometry. *Nucleic Acids Res.* **2002**, *30* (2), No. E7.
(14) Hofer, T.; Badouard, C.; Bajak, E.; Ravanat, J. L.; Mattsson, A.; Cotgreave, I. A. Hydrogen peroxide causes greater oxidation in cellular RNA than in DNA. *Biol. Chem.* **2005**, *386* (4), 333−337.
(15) Hofer, T.; Seo, A. Y.; Prudencio, M.; Leeuwenburgh, C. A method to determine RNA and DNA oxidation simultaneously by HPLC-ECD: greater RNA than DNA oxidation in rat liver after doxorubicin administration. *Biol. Chem.* **2006**, *387* (1), 103−111.
(16) Li, Z.; Wu, J.; Deleo, C. J. RNA damage and surveillance under oxidative stress. *IUBMB Life* **2006**, *58* (10), 581−588.
(17) Sun, C.; Jora, M.; Solivio, B.; Limbach, P. A.; Addepalli, B. The effects of ultraviolet radiation on nucleoside modifications in RNA. *ACS Chem. Biol.* **2018**, *13* (3), 567−572.
(18) Ishii, T.; Sekiguchi, M. Two ways of escaping from oxidative RNA damage: Selective degradation and cell death. *DNA Repair* **2019**, *81*, 102666.
(19) Li, Z.; Chen, X.; Liu, Z.; Ye, W.; Li, L.; Qian, L.; Ding, H.; Li, P.; Aung, L. H. H. Recent advances: Molecular mechanism of RNA oxidation and its role in various diseases. *Front. Mol. Biosci.* **2020**, *7*, 1−7.
(20) Sun, C.; Limbach, P. A.; Addepalli, B. Characterization of UVA-induced alterations to transfer RNA sequences. *Biomolecules* **2020**, *10* (11), 1527.
(21) Estevez, M.; Valesyan, S.; Jora, M.; Limbach, P. A.; Addepalli, B. Oxidative damage to RNA is altered by the presence of interacting proteins or modified nucleosides. *Front. Mol. Biosci.* **2021**, *8*, 697149.
(22) Fasnacht, M.; Polacek, N. Oxidative stress in bacteria and the central dogma of molecular biology. *Front. Mol. Biosci.* **2021**, *8*, 671037.
(23) Sapio, R. T.; Burns, C. J.; Pestov, D. G. Effects of hydrogen peroxide stress on the nucleolar redox environment and pre-rRNA maturation. *Front. Mol. Biosci.* **2021**, *8*, 678488.
(24) Tanaka, M.; Chock, P. B. Oxidative modifications of RNA and its potential roles in biosystem. *Front. Mol. Biosci.* **2021**, *8*, 685331.
(25) Chao, M.-R.; Evans, M. D.; Hu, C.-W.; Ji, Y.; Møller, P.; Rossner, P.; Cooke, M. S. Biomarkers of nucleic acid oxidation − A summary state-of-the-art. *Redox Biol.* **2021**, *42*, 101872.
(26) Cohn, W. E.; Volkin, E. Nucleoside-5′-phosphates from ribonucleic acid. *Nature* **1951**, *167* (4247), 483−484.
(27) Cohn, W. E. Pseudouridine, a carbon-carbon linked ribonucleoside in ribonucleic acids: isolation, structure, and chemical characteristics. *J. Biol. Chem.* **1960**, *235*, 1488−1498.
(28) Davis, F. F.; Allen, F. W. Ribonucleic acids from yeast which contain a fifth nucleotide. *J. Biol. Chem.* **1957**, *227* (2), 907−915.
(29) Yu, C. T.; Allen, F. W. Studies on an isomer of uridine isolated from ribonucleic acids. *Biochim. Biophys. Acta* **1959**, *32*, 393−406.
(30) Cohn, W. E. 5-Ribosyl uracil, a carbon-carbon ribofuranosyl nucleoside in ribonucleic acids. *Biochim. Biophys. Acta* **1959**, *32* (2), 569−571.
(31) Machnicka, M. A.; Milanowska, K.; Osman Oglou, O.; Purta, E.; Kurkowska, M.; Olchowik, A.; Januszewski, W.; Kalinowski, S.; Dunin-Horkawicz, S.; Rother, K. M.; et al. MODOMICS: a database of RNA modification pathways–2013 update. *Nucleic Acids Res.* **2012**, *41* (D1), D262−D267.
(32) Boccaletto, P.; Stefaniak, F.; Ray, A.; Cappannini, A.; Mukherjee, S.; Purta, E.; Kurkowska, M.; Shirvanizadeh, N.; Destefanis, E.; Groza, P.; et al. MODOMICS: a database of RNA modification pathways. 2021 update. *Nucleic Acids Res.* **2022**, *50* (D1), D231−D235.
(33) Delaunay, S.; Helm, M.; Frye, M. RNA modifications in physiology and disease: towards clinical applications. *Nat. Rev. Genet.* **2024**, *25* (2), 104−122.
(34) Limbach, P. A.; Crain, P. F.; McCloskey, J. A. Summary: the modified nucleosides of RNA. *Nucleic Acids Res.* **1994**, *22* (12), 2183−2196.
(35) Limbach, P. A.; Crain, P. F.; Pomerantz, S. C.; McCloskey, J. A. Structures of posttranscriptionally modified nucleosides from RNA. *Biochimie* **1995**, *77* (1−2), 135−138.
(36) Crain, P. F.; McCloskey, J. A. The RNA modification database. *Nucleic Acids Res.* **1997**, *25* (1), 126−127.
(37) Pang, H.; Smith, D. L.; Crain, P. F.; Yamaizumi, K.; Nishimura, S.; McCloskey, J. A. Identification of nucleosides in hydrolysates of transfer RNA by high-resolution mass spectrometry. *Eur. J. Biochem.* **1982**, *127* (3), 459−471.
(38) McCloskey, J. A. Electron ionization mass spectra of trimethylsilyl derivatives of nucleosides. *Methods Enzymol.* **1990**, *193*, 825−842.

https://doi.org/10.1021/acsomega.4c09310
ACS Omega 2025, 10, 1519−1530

(39) Mccloskey, J. A. Structural characterization of natural nucleosides by mass spectrometry. *Acc. Chem. Res.* **1991**, *24* (3), 81−88.
(40) Limbach, P. A.; Crain, P. F.; McCloskey, J. A. Characterization of oligonucleotides and nucleic acids by mass spectrometry. *Curr. Opin. Biotechnol.* **1995**, *6* (1), 96−102.
(41) Takeshita, T.; Kanaly, R. A. In vitro DNA/RNA adductomics to confirm DNA damage caused by benzo[a]pyrene in the Hep G2 cell line. *Front. Chem.* **2019**, *7*, 491.
(42) Zhang, L.; Zhang, W.; Wang, H. Accurate quantification of ten methylated purine nucleosides by highly sensitive and stable isotope-diluted UHPLC-MS/MS. *Anal. Chem.* **2024**, *96* (28), 11366−11373.
(43) Taghizadeh, K.; McFaline, J. L.; Pang, B.; Sullivan, M.; Dong, M.; Plummer, E.; Dedon, P. C. Quantification of DNA damage products resulting from deamination, oxidation and reaction with products of lipid peroxidation by liquid chromatography isotope dilution tandem mass spectrometry. *Nat. Protoc.* **2008**, *3* (8), 1287−1298.
(44) Murphy, M. P.; Bayir, H.; Belousov, V.; Chang, C. J.; Davies, K. J. A.; Davies, M. J.; Dick, T. P.; Finkel, T.; Forman, H. J.; Janssen-Heininger, Y.; et al. Guidelines for measuring reactive oxygen species and oxidative damage in cells and in vivo. *Nat. Metab.* **2022**, *4* (6), 651−662.
(45) Zhang, J.; Perry, G.; Smith, M. A.; Robertson, D.; Olson, S. J.; Graham, D. G.; Montine, T. J. Parkinson's disease is associated with oxidative damage to cytoplasmic DNA and RNA in substantia nigra neurons. *Am. J. Pathol.* **1999**, *154* (5), 1423−1429.
(46) Nunomura, A.; Perry, G.; Hirai, K.; Aliev, G.; Takeda, A.; Chiba, S.; Smith, M. A. Neuronal RNA oxidation in Alzheimer's disease and Down's syndrome. *Ann. N.Y. Acad. Sci.* **1999**, *893*, 362−364.
(47) Nunomura, A.; Perry, G.; Pappolla, M. A.; Wade, R.; Hirai, K.; Chiba, S.; Smith, M. A. RNA oxidation is a prominent feature of vulnerable neurons in Alzheimer's disease. *J. Neurosci.* **1999**, *19* (6), 1959−1964.
(48) Honda, K.; Smith, M. A.; Zhu, X.; Baus, D.; Merrick, W. C.; Tartakoff, A. M.; Hattier, T.; Harris, P. L.; Siedlak, S. L.; Fujioka, H.; et al. Ribosomal RNA in Alzheimer disease is oxidized by bound redox-active iron. *J. Biol. Chem.* **2005**, *280* (22), 20978−20986.
(49) Ding, Q.; Markesbery, W. R.; Cecarini, V.; Keller, J. N. Decreased RNA, and increased RNA oxidation, in ribosomes from early Alzheimer's disease. *Neurochem. Res.* **2006**, *31* (5), 705−710.
(50) Hofer, T.; Marzetti, E.; Xu, J.; Seo, A. Y.; Gulec, S.; Knutson, M. D.; Leeuwenburgh, C.; Dupont-Versteegden, E. E. Increased iron content and RNA oxidative damage in skeletal muscle with aging and disuse atrophy. *Exp. Gerontol.* **2008**, *43* (6), 563−570.
(51) Castellani, R. J.; Nunomura, A.; Rolston, R. K.; Moreira, P. I.; Takeda, A.; Perry, G.; Smith, M. A. Sublethal RNA oxidation as a mechanism for neurodegenerative disease. *Int. J. Mol. Sci.* **2008**, *9* (5), 789−806.
(52) Kong, Q.; Lin, C. L. Oxidative damage to RNA: mechanisms, consequences, and diseases. *Cell. Mol. Life Sci.* **2010**, *67* (11), 1817−1829.
(53) Nunomura, A.; Moreira, P. I.; Castellani, R. J.; Lee, H. G.; Zhu, X.; Smith, M. A.; Perry, G. Oxidative damage to RNA in aging and neurodegenerative disorders. *Neurotoxic. Res.* **2012**, *22* (3), 231−248.
(54) Nunomura, A.; Tamaoki, T.; Motohashi, N.; Nakamura, M.; McKeel, D. W.; Tabaton, M.; Lee, H. G.; Smith, M. A.; Perry, G.; Zhu, X. The earliest stage of cognitive impairment in transition from normal aging to Alzheimer disease is marked by prominent RNA oxidation in vulnerable neurons. *J. Neuropathol. Exp. Neurol.* **2012**, *71* (3), 233−241.
(55) Poulsen, H. E.; Specht, E.; Broedbaek, K.; Henriksen, T.; Ellervik, C.; Mandrup-Poulsen, T.; Tonnesen, M.; Nielsen, P. E.; Andersen, H. U.; Weimann, A. RNA modifications by oxidation: a novel disease mechanism? *Free Radical Biol. Med.* **2012**, *52* (8), 1353−1361.
(56) Fimognari, C. Role of Oxidative RNA Damage in Chronic-Degenerative Diseases. *Oxid. Med. Cell. Longevity* **2015**, *2015*, 358713.
(57) Jacoby, A. S.; Vinberg, M.; Poulsen, H. E.; Kessing, L. V.; Munkholm, K. Increased DNA and RNA damage by oxidation in patients with bipolar I disorder. *Transl. Psychiatry* **2016**, *6* (8), No. e867.
(58) Nunomura, A.; Lee, H. G.; Zhu, X.; Perry, G. Consequences of RNA oxidation on protein synthesis rate and fidelity: implications for the pathophysiology of neuropsychiatric disorders. *Biochem. Soc. Trans.* **2017**, *45* (5), 1053−1066.
(59) Liguori, I.; Russo, G.; Curcio, F.; Bulli, G.; Aran, L.; Della-Morte, D.; Gargiulo, G.; Testa, G.; Cacciatore, F.; Bonaduce, D.; et al. Oxidative stress, aging, and diseases. *Clin. Interventions Aging* **2018**, *13*, 757−772.
(60) Willi, J.; Kupfer, P.; Evequoz, D.; Fernandez, G.; Katz, A.; Leumann, C.; Polacek, N. Oxidative stress damages rRNA inside the ribosome and differentially affects the catalytic center. *Nucleic Acids Res.* **2018**, *46* (4), 1945−1957.
(61) Cejvanovic, V.; Kjaer, L. K.; Morup Bergholdt, H. K.; Henriksen, T.; Weimann, A.; Ellervik, C.; Poulsen, H. E. RNA oxidation and iron levels in patients with diabetes. *Free Radical Biol. Med.* **2018**, *129*, 532−536.
(62) Yan, L. L.; Zaher, H. S. How do cells cope with RNA damage and its consequences? *J. Biol. Chem.* **2019**, *294* (41), 15158−15171.
(63) Seok, H.; Lee, H.; Lee, S.; Ahn, S. H.; Lee, H. S.; Kim, G. D.; Peak, J.; Park, J.; Cho, Y. K.; Jeong, Y.; et al. Position-specific oxidation of miR-1 encodes cardiac hypertrophy. *Nature* **2020**, *584* (7820), 279−285.
(64) Barbieri, I.; Kouzarides, T. Role of RNA modifications in cancer. *Nat. Rev. Cancer* **2020**, *20* (6), 303−322.
(65) Chen, X.; Yu, H.; Li, Z.; Ye, W.; Liu, Z.; Gao, J.; Wang, Y.; Li, X.; Zhang, L.; Alenina, N.; et al. Oxidative RNA damage in the pathogenesis and treatment of type 2 diabetes. *Front. Physiol.* **2022**, *13*, 725919.
(66) Luo, T.; Huo, C.; Zhou, T.; Xie, S. Progress on RNA-based therapeutics for genetic diseases. *Zhejiang Daxue Xuebao, Yixueban* **2023**, *52* (4), 406−416.
(67) Jorgensen, A.; Brandslund, I.; Ellervik, C.; Henriksen, T.; Weimann, A.; Andersen, P. K.; Poulsen, H. E. Specific prediction of mortality by oxidative stress-induced damage to RNA vs. DNA in humans. *Aging Cell* **2023**, *22* (6), No. e13839.
(68) Coello, K.; Makinen, I. J. O.; Kjaerstad, H. L.; Faurholt-Jepsen, M.; Miskowiak, K. W.; Poulsen, H. E.; Vinberg, M.; Kessing, L. V. Oxidation of DNA and RNA in young patients with newly diagnosed bipolar disorder and relatives. *Transl. Psychiatry* **2024**, *14* (1), 81.
(69) Stafforst, T.; Schneider, M. F. An RNA-deaminase conjugate selectively repairs point mutations. *Angew. Chem., Int. Ed. Engl.* **2012**, *51* (44), 11166−11169.
(70) Montiel-Gonzalez, M. F.; Vallecillo-Viejo, I.; Yudowski, G. A.; Rosenthal, J. J. Correction of mutations within the cystic fibrosis transmembrane conductance regulator by site-directed RNA editing. *Proc. Natl. Acad. Sci. U.S.A.* **2013**, *110* (45), 18285−18290.
(71) Matthews, M. M.; Thomas, J. M.; Zheng, Y.; Tran, K.; Phelps, K. J.; Scott, A. I.; Havel, J.; Fisher, A. J.; Beal, P. A. Structures of human ADAR2 bound to dsRNA reveal base-flipping mechanism and basis for site selectivity. *Nat. Struct. Mol. Biol.* **2016**, *23* (5), 426−433.
(72) Abudayyeh, O. O.; Gootenberg, J. S.; Franklin, B.; Koob, J.; Kellner, M. J.; Ladha, A.; Joung, J.; Kirchgatterer, P.; Cox, D. B. T.; Zhang, F. A cytosine deaminase for programmable single-base RNA editing. *Science* **2019**, *365* (6451), 382−386.
(73) Chen, G.; Katrekar, D.; Mali, P. RNA-Guided Adenosine Deaminases: Advances and Challenges for Therapeutic RNA Editing. *Biochemistry* **2019**, *58* (15), 1947−1957.
(74) Katrekar, D.; Chen, G.; Meluzzi, D.; Ganesh, A.; Worlikar, A.; Shih, Y. R.; Varghese, S.; Mali, P. In vivo RNA editing of point mutations via RNA-guided adenosine deaminases. *Nat. Methods* **2019**, *16* (3), 239−242.
(75) Crooke, S. T.; Baker, B. F.; Crooke, R. M.; Liang, X. H. Antisense technology: an overview and prospectus. *Nat. Rev. Drug Discovery* **2021**, *20* (6), 427−453.

https://doi.org/10.1021/acsomega.4c09310
ACS Omega 2025, 10, 1519−1530

(76) Zhu, Y.; Zhu, L.; Wang, X.; Jin, H. RNA-based therapeutics: an overview and prospectus. *Cell Death Dis.* **2022**, *13* (7), 644.
(77) Sparmann, A.; Vogel, J. RNA-based medicine: from molecular mechanisms to therapy. *EMBO J.* **2023**, *42* (21), No. e114760.
(78) Relier, S.; Amalric, A.; Attina, A.; Koumare, I. B.; Rigau, V.; Burel Vandenbos, F.; Fontaine, D.; Baroncini, M.; Hugnot, J. P.; Duffau, H.; et al. Multivariate Analysis of RNA Chemistry Marks Uncovers Epitranscriptomics-Based Biomarker Signature for Adult Diffuse Glioma Diagnostics. *Anal. Chem.* **2022**, *94* (35), 11967−11972.
(79) Lee, R. C.; Feinbaum, R. L.; Ambros, V. The C. elegans heterochronic gene lin-4 encodes small RNAs with antisense complementarity to lin-14. *Cell* **1993**, *75* (5), 843−854.
(80) Wightman, B.; Ha, I.; Ruvkun, G. Posttranscriptional regulation of the heterochronic gene lin-14 by lin-4 mediates temporal pattern formation in C. elegans. *Cell* **1993**, *75* (5), 855−862.
(81) Shang, R.; Lee, S.; Senavirathne, G.; Lai, E. C. microRNAs in action: biogenesis, function and regulation. *Nat. Rev. Genet.* **2023**, *24* (12), 816−833.
(82) Nick McElhinny, S. A.; Watts, B. E.; Kumar, D.; Watt, D. L.; Lundstrom, E. B.; Burgers, P. M.; Johansson, E.; Chabes, A.; Kunkel, T. A. Abundant ribonucleotide incorporation into DNA by yeast replicative polymerases. *Proc. Natl. Acad. Sci. U.S.A.* **2010**, *107* (11), 4949−4954.
(83) McElhinny, S. A. N.; Kumar, D.; Clark, A. B.; Watt, D. L.; Watts, B. E.; Lundstrom, E.-B.; Johansson, E.; Chabes, A.; Kunkel, T. A. Genome instability due to ribonucleotide incorporation into DNA. *Nat. Chem. Biol.* **2010**, *6* (10), 774−781.
(84) Reijns, M. A.; Rabe, B.; Rigby, R. E.; Mill, P.; Astell, K. R.; Lettice, L. A.; Boyle, S.; Leitch, A.; Keighren, M.; Kilanowski, F.; et al. Enzymatic removal of ribonucleotides from DNA is essential for mammalian genome integrity and development. *Cell* **2012**, *149* (5), 1008−1022.
(85) Williams, J. S.; Lujan, S. A.; Kunkel, T. A. Processing ribonucleotides incorporated during eukaryotic DNA replication. *Nat. Rev. Mol. Cell Biol.* **2016**, *17* (6), 350−363.
(86) Lujan, S. A.; Williams, J. S.; Clausen, A. R.; Clark, A. B.; Kunkel, T. A. Ribonucleotides are signals for mismatch repair of leading-strand replication errors. *Mol. Cell* **2013**, *50* (3), 437−443.
(87) Ghodgaonkar, M. M.; Lazzaro, F.; Olivera-Pimentel, M.; Artola-Boran, M.; Cejka, P.; Reijns, M. A.; Jackson, A. P.; Plevani, P.; Muzi-Falconi, M.; Jiricny, J. Ribonucleotides misincorporated into DNA act as strand-discrimination signals in eukaryotic mismatch repair. *Mol. Cell* **2013**, *50* (3), 323−332.
(88) Williams, J. S.; Kunkel, T. A. Ribonucleotides in DNA: origins, repair and consequences. *DNA Repair* **2014**, *19*, 27−37.
(89) Cerritelli, S. M.; Crouch, R. J. The balancing act of ribonucleotides in DNA. *Trends Biochem. Sci.* **2016**, *41* (5), 434−445.
(90) Hawley, B. R.; Lu, W. T.; Wilczynska, A.; Bushell, M. The emerging role of RNAs in DNA damage repair. *Cell Death Differ.* **2017**, *24* (4), 580−587.
(91) Pryor, J. M.; Conlin, M. P.; Carvajal-Garcia, J.; Luedeman, M. E.; Luthman, A. J.; Small, G. W.; Ramsden, D. A. Ribonucleotide incorporation enables repair of chromosome breaks by nonhomologous end joining. *Science* **2018**, *361* (6407), 1126−1129.
(92) Tsao, N.; Ashour, M. E.; Mosammaparast, N. How RNA impacts DNA repair. *DNA Repair* **2023**, *131*, 103564.
(93) National Academies of Sciences, Engineering, and Medicine *Charting a Future for Sequencing RNA and Its Modifications: A New Era for Biology and Medicine*; The National Academies Press: DC, 2024.
(94) Alexander, A. J.; Kebarle, P.; Fuciarelli, A. F.; Raleigh, J. A. Characterization of radiation-induced damage to polyadenylic acid using high-performance liquid chromatography tandem mass spectrometry. *Anal. Chem.* **1987**, *59* (20), 2484−2491.
(95) Wurtmann, E. J.; Wolin, S. L. RNA under attack: cellular handling of RNA damage. *Crit. Rev. Biochem. Mol. Biol.* **2009**, *44* (1), 34−49.
(96) Broedbaek, K.; Poulsen, H. E.; Weimann, A.; Kom, G. D.; Schwedhelm, E.; Nielsen, P.; Boger, R. H. Urinary excretion of biomarkers of oxidatively damaged DNA and RNA in hereditary hemochromatosis. *Free Radical Biol. Med.* **2009**, *47* (8), 1230−1233.
(97) Henriksen, T.; Hillestrom, P. R.; Poulsen, H. E.; Weimann, A. Automated method for the direct analysis of 8-oxo-guanosine and 8-oxo-2'-deoxyguanosine in human urine using ultraperformance liquid chromatography and tandem mass spectrometry. *Free Radical Biol. Med.* **2009**, *47* (5), 629−635.
(98) Hu, C. W.; Chao, M. R.; Sie, C. H. Urinary analysis of 8-oxo-7,8-dihydroguanine and 8-oxo-7,8-dihydro-2'-deoxyguanosine by isotope-dilution LC-MS/MS with automated solid-phase extraction: Study of 8-oxo-7,8-dihydroguanine stability. *Free Radical Biol. Med.* **2010**, *48* (1), 89−97.
(99) Poulsen, H. E.; Nadal, L. L.; Broedbaek, K.; Nielsen, P. E.; Weimann, A. Detection and interpretation of 8-oxodG and 8-oxoGua in urine, plasma and cerebrospinal fluid. *Biochim. Biophys. Acta* **2014**, *1840* (2), 801−808.
(100) Munkholm, K.; Poulsen, H. E.; Kessing, L. V.; Vinberg, M. Elevated levels of urinary markers of oxidatively generated DNA and RNA damage in bipolar disorder. *Bipolar Disord.* **2015**, *17* (3), 257−268.
(101) Hu, C. W.; Cooke, M. S.; Tsai, Y. H.; Chao, M. R. 8-Oxo-7,8-dihydroguanine and 8-oxo-7,8-dihydro-2'-deoxyguanosine concentrations in various human body fluids: implications for their measurement and interpretation. *Arch. Toxicol.* **2015**, *89* (2), 201−210.
(102) Henriksen, T.; Weimann, A.; Larsen, E. L.; Poulsen, H. E. Quantification of 8-oxo-7,8-dihydro-2'-deoxyguanosine and 8-oxo-7,8-dihydro-guanosine concentrations in urine and plasma for estimating 24-h urinary output. *Free Radical Biol. Med.* **2021**, *172*, 350−357.
(103) Phillips, C. N.; Schowe, S.; Langeberg, C. J.; Siddique, N.; Chapman, E. G.; Resendiz, M. J. E. Processing of RNA containing 8-oxo-7,8-dihydroguanosine (8-oxoG) by the exoribonuclease Xrn-1. *Front. Mol. Biosci.* **2021**, *8*, 780315.
(104) Dizdaroglu, M.; Jaruga, P.; Rodriguez, H. Identification and quantification of 8,5′-cyclo-2'-deoxyadenosine in DNA by liquid chromatography/mass spectrometry. *Free Radical Biol. Med.* **2001**, *30* (7), 774−784.
(105) Jaruga, P.; Birincioglu, M.; Rodriguez, H.; Dizdaroglu, M. Mass spectrometric assays for the tandem lesion 8,5′-cyclo-2'-deoxyguanosine in mammalian DNA. *Biochemistry* **2002**, *41* (11), 3703−3711.
(106) Tuo, J. S.; Jaruga, P.; Rodriguez, H.; Dizdaroglu, M.; Bohr, V. A. The Cockayne syndrome group B gene product is involved in cellular repair of 8-hydroxyadenine in DNA. *J. Biol. Chem.* **2002**, *277* (34), 30832−30837.
(107) Birincioglu, M.; Jaruga, P.; Chowdhury, G.; Rodriguez, H.; Dizdaroglu, M.; Gates, K. S. DNA base damage by the antitumor agent 3-amino-1,2,4-benzotriazine 1,4-dioxide (tirapazamine). *J. Am. Chem. Soc.* **2003**, *125* (38), 11607−11615.
(108) Berger, M.; Cadet, J. Isolation and characterization of the radiation-induced degradation products of 2′-deoxyguanosine in oxygen-free aqueous solutions. *Z. Naturforsch., B: J. Chem. Sci.* **1985**, *40* (11), 1519−1531.
(109) Raoul, S.; Bardet, M.; Cadet, J. Gamma irradiation of 2′-deoxyadenosine in oxygen-free aqueous solutions: identification and conformational features of formamidopyrimidine nucleoside derivatives. *Chem. Res. Toxicol.* **1995**, *8* (7), 924−933.
(110) Greenberg, M. M.; Hantosi, Z.; Wiederholt, C. J.; Rithner, C. D. Studies on N4-(2-deoxy-d-pentofuranosyl)-4,6-diamino-5-formamidopyrimidine (Fapy.dA) and N6-(2-deoxy-d-pentofuranosyl)-6-diamino-5-formamido-4-hydroxypyrimidine (Fapy.dG). *Biochemistry* **2001**, *40* (51), 15856−15861.
(111) Burgdorf, L. T.; Carell, T. Synthesis, stability, and conformation of the formamidopyrimidine G DNA lesion. *Chem. - Eur. J.* **2002**, *8* (1), 293−301.
(112) Patro, J. N.; Haraguchi, K.; Delaney, M. O.; Greenberg, M. M. Probing the configurations of formamidopyrimidine lesions Fapy.dA and Fapy.dG in DNA using endonuclease IV. *Biochemistry* **2004**, *43* (42), 13397−13403.

https://doi.org/10.1021/acsomega.4c09310
ACS Omega 2025, 10, 1519−1530

(113) Cavalieri, L. F.; Bendich, A. The ultraviolet absorption spectra of pyrimidines and purines. *J. Am. Chem. Soc.* **1950**, *72* (6), 2587−2594.
(114) Frelon, S.; Douki, T.; Ravanat, J. L.; Pouget, J. P.; Tornabene, C.; Cadet, J. High-performance liquid chromatography–tandem mass spectrometry measurement of radiation-induced base damage to isolated and cellular DNA. *Chem. Res. Toxicol.* **2000**, *13* (10), 1002−1010.
(115) Hogenkamp, H. P. C. A cyclic nucleoside derived from coenzyme B12. *J. Biol. Chem.* **1963**, *238* (1), 477−480.
(116) Keck, K. Bildung von Cyclonucleotiden bei Bestrahlung wäßriger Lüsungen von Purinnucleotiden. *Z. Naturforsch.* **1968**, *23*, 1034−1043.
(117) Kasai, H.; Nishimura, S. Hydroxylation of deoxyguanosine at the C-8 position by ascorbic acid and other reducing agents. *Nucleic Acids Res.* **1984**, *12* (4), 2137−2145.
(118) Dizdaroglu, M. Formation of an 8-hydroxyguanine moiety in deoxyribonucleic acid on gamma-Irradiation in aqueous solution. *Biochemistry* **1985**, *24* (16), 4476−4481.
(119) Kant, M.; Jaruga, P.; Coskun, E.; Ward, S.; Stark, A. D.; Baumann, T.; Becker, D.; Adhikary, A.; Sevilla, M. D.; Dizdaroglu, M. Ne-22 ion-beam radiation damage to DNA: From initial free radical formation to resulting DNA-base damage. *ACS Omega* **2021**, *6* (25), 16600−16611.
(120) Jaruga, P.; Dizdaroglu, M. 8,5′-Cyclopurine-2′-deoxynucleosides in DNA: mechanisms of formation, measurement, repair and biological effects. *DNA Repair* **2008**, *7* (9), 1413−1425.
(121) Jaruga, P.; Rozalski, R.; Jawien, A.; Migdalski, A.; Olinski, R.; Dizdaroglu, M. DNA damage products (5′R)- and (5′S)-8,5′-cyclo-2′-deoxyadenosines as potential biomarkers in human urine for atherosclerosis. *Biochemistry* **2012**, *51* (9), 1822−1824.
(122) Pomerantz, S. C.; Mccloskey, J. A. Analysis of RNA hydrolyzates by liquid-chromatography mass spectrometry. *Methods Enzymol.* **1990**, *193*, 796−824.

https://doi.org/10.1021/acsomega.4c09310
ACS Omega 2025, 10, 1519−1530